AIP | Review of Scientific Instruments

Time-of-flight measurements of low-energy electron energy distributions from ion–atom collisions

L. H. Toburen and W. E. Wilson

Citation: Review of Scientific Instruments **46**, 851 (1975); doi: 10.1063/1.1134352
View online: http://dx.doi.org/10.1063/1.1134352
View Table of Contents: http://scitation.aip.org/content/aip/journal/rsi/46/7?ver=pdfcov
Published by the AIP Publishing

Time-of-flight measurements of low-energy electron energy distributions from ion–atom collisions*

L. H. Toburen and W. E. Wilson

Battelle Northwest Laboratory, Richland, Washington 99352

(Received 21 February 1975; in final form, 10 April 1975)

A time-of-flight technique for the measurement of the energy spectra of electrons ejected in ion–atom collisions is described. Ionization is produced by a pulsed beam of protons which are obtained by chopping the dc proton beam from a Van de Graaff accelerator with a 3.33 MHz high voltage oscillator. Electron energy and angular distributions are derived from time-of-flight spectra recorded for different emission angles. This system is capable of measurements for proton energies from 0.25 to 2.0 MeV, ejected electron energies from 0.3 eV to several hundred eV, and electron ejection angles from 30° to 150°. The advantages and limitations of this technique are illustrated.

I. INTRODUCTION

Although the ionization of atoms and molecules by fast charged particles and the resulting energy and angular distributions of ionized electrons are of great importance in many areas of physics, this process has been studied experimentally only recently.[1,2] The extensive programs conducted at the University of Nebraska, Hahn-Meitner Institute, and at Battelle Northwest to study the details of electron emission in ion–atom collisions have had one basic technique in common; all have used electrostatic analyzers for the measurement of electron energy spectra. Although the three laboratories cover a wide range of incident proton energies, each has made measurements at a common proton energy where a comparison of the results can be made. Such comparison for 0.3 MeV protons on nitrogen was first discussed by Stolterfoht.[3] It was shown that, although excellent agreement was found among the various measurements for electron energies greater than about 25 eV, large discrepancies were present for lower energy electrons. These discrepancies illustrate the inherent difficulties in measurements of low-energy electron distributions by electrostatic analyzers, where transmission through the analyzer is strongly affected by stray electric and/or magnetic fields. Although Stolterfoht[4] has recently improved his system and is in close agreement with Rudd *et al.*[2] to electron energies as low as 5 eV, there are still large uncertainties in the measurements at energies below 5 eV. These discrepancies, along with the need to know low-energy cross sections in order to test theoretical calculations and to obtain accurate total cross sections from the double-differential cross sections, motivated our development of the time-of-flight technique. Since this technique does not use electrostatic fields for energy analysis, effects due to fringing electric fields are not present, and short flight paths may be chosen in order to minimize the effects of residual magnetic fields.

II. INSTRUMENTATION

A schematic of the time-of-flight (TOF) electron energy analysis system is shown in Fig. 1. The proton beam obtained from a 2 MV Van de Graaff accelerator is momentum analyzed and focused to maximize the direct current through the collimators and into the Faraday cup. The first and second apertures shown in Fig. 1 are 1.27 mm in diameter and separated by approximately 20 cm. The apertures in the electron suppressor and shield as well as the Faraday cup are approximately 2.5 mm in diameter; these apertures are larger than the entrance collimators to insure minimum interaction of the proton beam with collimator edges. After the alignment and focus are optimized using the dc proton beam, the rf oscillator is energized. The crystal controlled oscillator operates at 3.33 MHz and provides a high voltage signal of about 40 kV peak-to-peak to a pair of vertical deflection plates. A set of horizontal deflection plates (not shown in Fig. 1) is supplied with a voltage shifted in phase by 90° relative to the vertical deflection voltage and thus allows only one proton pulse per cycle to pass through the collimators at the target chamber. The high writing speed generated by the high voltage oscillator coupled with the long distance between chopping plates and entrance collimator (approximately 3 m) provides a proton pulse width of less than 0.7 nsec (FWHM). Since this procedure does not include particle bunching, a factor of nearly 1000 in time average beam intensity is lost in going from dc to pulsed beam configuration. High loss in average beam current has not been found to be a limiting factor in the measurements.

The interaction region is formed by the intersection of the pulsed proton beam and a directed-flow gas beam target. The gas beam is formed by allowing gas to diffuse through a commercially available channel plate[5] consisting of nearly 2×10^5 holes, each with a length-to-diameter ratio of 100. The gas beam is directed into a cold-trapped diffusion pump which is placed approximately 15 cm directly below the channel plate. In addition, cylindrical baffles not shown in Fig. 1 are positioned immediately below the interaction region to help direct the gas into the diffusion pump. The actual target gas pressure in the interaction region is not known, however, calculations based on the conductance of the channel plate indicate that the pressure during opera-

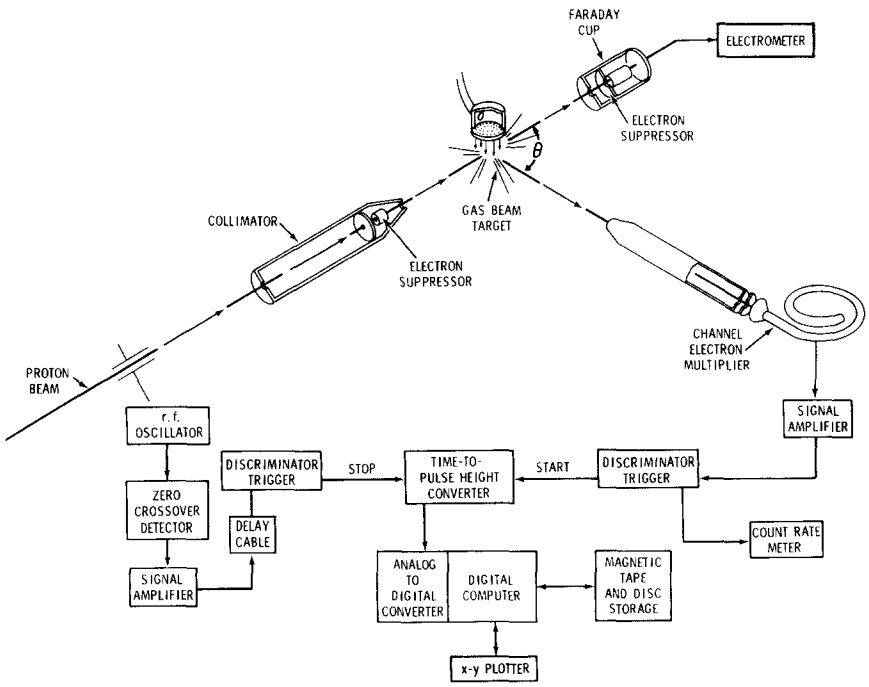

FIG. 1. Schematic of the time-of-flight apparatus and associated instrumentation.

tion is approximately 3×10^{-4} Torr in the vicinity of the proton beam. The pressure in the region of the electron multiplier and Faraday cup is measured to be approximately 3×10^{-5} during operation and 1×10^{-6} with the gas beam shut off. From an operational point of view, it is important to maintain adequate target density to provide usable electron count rates and yet maintain sufficiently low pressures so that electrons are not scattered by residual gas atoms in drifting from the interaction region to the electron detector. It appears that the present configuration produces a target gas density of approximately a factor of 10 greater in the interaction region than in the surrounding volume. The actual density profile within the gas beam has not been measured, since we are interested only in the relative yield of electrons and not in a direct measurement of the absolute cross sections. Absolute cross sections are obtained by normalization of the TOF results to previously measured absolute values; the normalization is made for ejected electron energies greater than 30 eV, where electrostatic analysis is reliable.

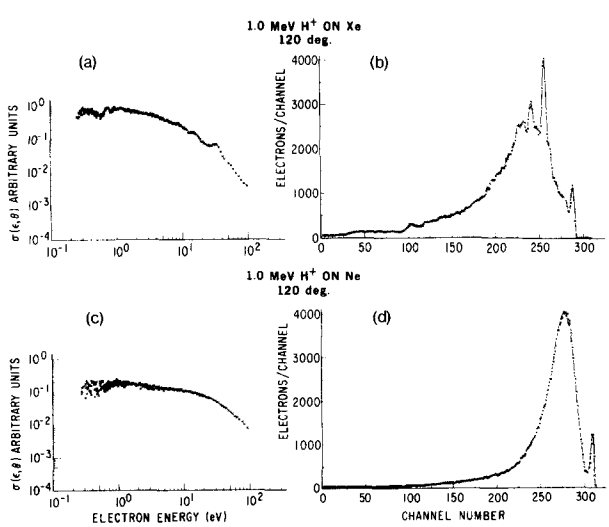

FIG. 2. Time-of-flight spectra for 1 MeV protons on Xe (b) and Ne (d) measured for electron ejection at 120°. The corresponding energy spectra derived from the time spectra are shown for Xe (a) and Ne (c).

Electrons ejected in collisions between the pulsed proton beam and the gas target are detected by a channel electron multiplier as a function of time following the proton pulse. The flight path is defined by apertures in the collimator preceding the electron detector. Not shown in Fig. 1 is an electrostatic shield which, except for the entrance aperture, completely enclosed the electron multiplier. This shield serves two purposes: (1) it screens the interaction region from the high voltages applied to the detector, and (2) it shields the detector from stray electrons insuring that only electrons which enter through the geometry defined by the collimators of the flight path are counted. In order to ensure optimum detection efficiency, a small accelerating potential is applied to the electrons immediately preceding the electron multiplier. This potential (normally 50 V) can be varied from 0 to 100 V without changing the shape of the measured electron spectra. This insensitivity of the electron spectra to accelerating voltage is evidence that the detector efficiency is constant for this type of electron detector for incident electrons from a few tenths of an electron volt to a few hundred electron volts.

The electronic instrumentation is also shown schematically in Fig. 1. The electron pulses from the electron multiplier are amplified by a wide band amplifier and shaped by a fast trigger circuit. The output of the trigger is used as the start signal of a time-to-pulse-height converter. The stop signal is derived from the high voltage oscillator which produces the pulsed proton beam. The stop signal is initiated by a crossover detector as the oscillator voltage passes through zero. This signal is amplified, delayed, and shaped by a trigger network to become the stop pulse. The pulse-height distribution corresponding to the time distribution of electrons arriving at the detector is recorded by an

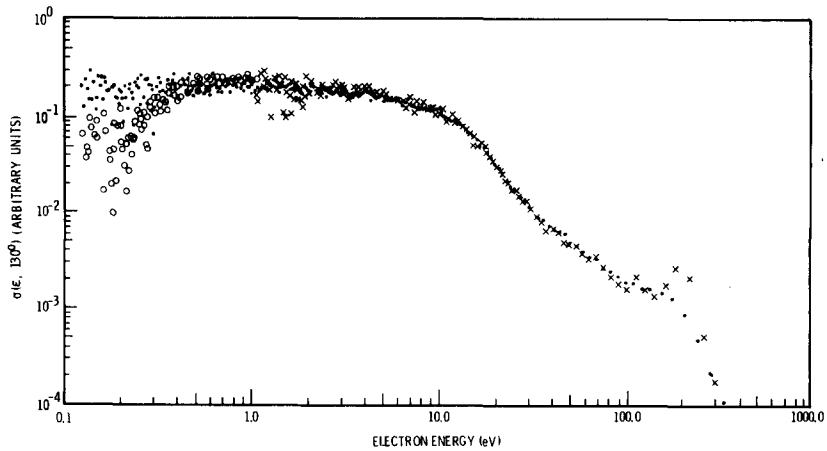

FIG. 3. Time-of-flight spectra obtained at 130° for 1 MeV protons on Ar. Data from two different path lengths are compared. ×—15 cm path length; ●, ○—7.5 cm path length.

analog-to-digital converter and stored in a small computer. The computer is used to convert the time spectrum to an energy spectrum which is plotted for comparison to energy spectra obtained from electrostatic energy analysis.

One of the primary difficulties in the measurement of low-energy electron distributions is the large influence of residual magnetic fields on these distributions. In the present system the entire vacuum chamber is surrounded by a double-walled magnetic shield. This shield, which is approximately 65 cm in diameter and 250 cm long, is supplemented with electric coils to further reduce the field. Magnetic field measurements indicate that a magnetic flux density of less than 2 mG exists in the interaction region after field nullification.

III. EXPERIMENTAL RESULTS AND ANALYSIS

Electron time-of-flight spectra and the corresponding energy distributions are shown in Fig. 2 for 1 MeV proton ionization of xenon and neon. The TOF spectra are on the right with the corresponding energy spectrum on the left. These spectra were obtained for electrons ejected at 120° with respect to the forward direction of the proton beam. The electron energy spectra are plotted for electron energies as low as 0.2 eV although, as will be discussed later, results for electron energies less than 0.5 eV are questionable due to uncertainties in assessing the background contributions. The peak on the right edge of the TOF spectra is produced by photons which arrive promptly after excitation of the target atom by the proton pulse. The difference in the channel location of this peak between the two spectra shown in Fig. 2 is due to a change in the length of delay cable used to delay the stop pulse. This prompt photon peak provides a reference marker for time, $t=0$, as well as a measure of the time resolution of the detection system. From a measure of the width of the photon peak we find that our present time resolution is approximately 3.5 nsec (FWHM). It is this time resolution which limits the energy resolution of our system. For example, the N-Auger transitions in Xe produce electrons of approximately 32 eV, which means they take about 30 nsec to travel the 7.5-cm path length to the detector. Thus the resolution is characteristically 10% for this energy region. Therefore, the N-Auger peak width observed at approximately channel 255 in the Xe spectrum arises from the system resolution and not the line widths of the Auger transitions. At lower electron energies, however, the energy resolution is much better. The peak observed at channel 100 in the Xe spectrum corresponds to an electron energy of approximately 1 eV, and the peak width is observed to be approximately 0.1 eV, of which the instrumental contribution is approximately 0.05 eV. It should be noted that these parameters are all characteristic of a flight path of 7.5 cm which was used to obtain the results shown in Fig. 2. The energy resolution can be improved by making the path length longer (at the expense of greater effects due to residual magnetic fields) or by improving the timing capabilities of the detection system. We feel that using a faster electron detector would probably be the most fruitful way to improve the energy response of the system. Attempts are presently underway to push the time resolution into the sub-nanosecond range.

The spectrum of Xe, which has a great deal of structure from Auger transitions and autoionization, is contrasted in Fig. 2 with the much smoother spectrum of Ne in order to demonstrate the potential of the TOF method for structure studies and to show that the Xe structure is not simply instrumental. The normal autoionization and Auger transitions of Ne occur at higher energies than for Xe and, since the energy resolution becomes poor at higher energies, the Ne lines are lost in the continuum background. Since the two spectra shown in Fig. 2 were taken under similar experimental conditions, it becomes evident that the low energy structure in Xe, which occurs between channels 25 and 150 in the TOF spectrum, is real and not due to scattered electrons. Scattered electrons would be independent of target structure and would also have occurred in the Ne spectrum. The low-energy electron lines in Xe have tentatively been identified as resulting from autoionizing transitions from Rydberg levels between $P_{\frac{3}{2}}$ and $P_{\frac{1}{2}}$ continua in Xe.[6] Further investigation of this phenomenon is now in progress.

In order to investigate the effects of magnetic fields on the electron distributions, measurements were made using two different flight distances. Since the effect of the magnetic field is dependent on both field magnitude and the length of path over which the field acts, one can be reasonably confident that magnetic field effects are negligible if the spectra are path length independent. The results of this investigation are shown in Fig. 3 for 1.0 MeV proton

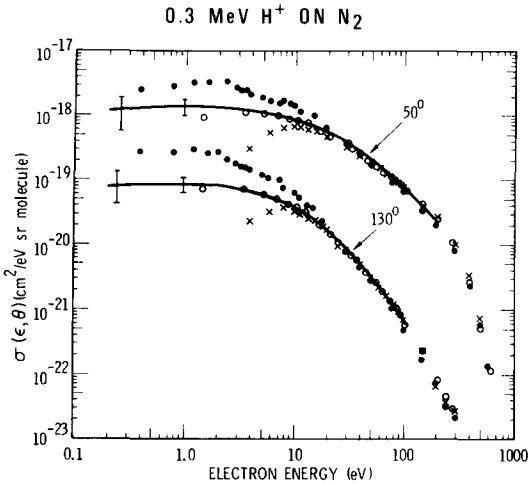

FIG. 4. A comparison of the time-of-flight results to previous electrostatic measurements. The TOF results are normalized to the electrostatic results at 50 eV. The electrostatic results are absolute measurements with no normalization performed; the results of Crooks and Rudd are from Ref. 8, the results of Stolterfoht are from Ref. 3, and the results of Toburen are from Ref. 9. —TOF; ●—Stolterfoht; ○—Crooks and Rudd; ×—Toburen.

ionization of Ar. The minimum energy which can be measured by TOF with our 3.33 MHz chopped beam is determined by the distance an electron can drift in 300 nsec, which is the time between pulses. For a 15.0 cm flight path electrons can be detected with energies down to approximately 1 eV; with the 7.5 cm path length electrons with energies as low as 0.1 eV are measurable. From the comparison shown in Fig. 3 we find excellent agreement for the two different flight paths where the spectra overlap. The lowest energy data with each path length show a great deal of scatter due to poor signal-to-background ratios and poor counting statistics. As can be seen in Fig. 2, the TOF count rate decreases as the electron energy decreases below 20 eV, and it is difficult to determine at what point the signal rate merges into and becomes dominated by background. However, it appears that realistic approximations for the background do not affect the electron spectra above about 0.3 eV. In Fig. 3 are shown two sets of data from the 7.5 cm path length TOF measurement analyzed assuming different background count rates. From this comparison it is obvious that data for electron energies smaller than about 0.3 eV are strongly influenced by uncertainties in the background counting rates. For this reason we tend to treat 0.3 eV as a lower limit to our energy range. Due to these uncertainties further development of the technique will be necessary in order to push the limit to lower electron energies. However, the lower limit of 0.3 eV for measurement of accurate electron energy distributions is a significant improvement in technique in view of previous measurements which were questionable at energies nearly two orders of magnitude larger.

In any measurement of electron energy spectra it is difficult to obtain a precise calibration of the energy scale, and this is particularly true for very low-energy electrons where contact potentials may be important. The energy scale used in our TOF measurements is based on the time-of-arrival of an electron over a known flight distance, with time $t_0=0$ being determined from the time of arrival of the "prompt" photon associated with excitation of the target atom or molecule. Contact potentials must be considered in these measurements because the electrons are ejected from target atoms or molecules in close proximity to the stainless steel collimated holes structure and then enter brass collimators preceding the detector. Since the target gas diffuser and the electron collimator are integrally connected through a support structure, one may expect the electrons to gain as much as 0.24 eV before arriving in the field free region of the collimator; 0.24 V is the contact potential between iron and brass. This 0.24 eV correction to the electron energies which are obtained from the known arrival time of electrons and known path length provides agreement to ± 0.1 eV between measured structure in Xe and both NOO Auger transition energies given by Seigbahn *et al.*,[7] and autoionization lines inferred from photoabsorption data of Comes *et al.*[6] These results for Xe which cover the energy range 0.34–35 eV will be discussed in detail in a future publication.

The primary incentive for the development of this TOF system was to resolve the discrepancies in reported low-energy electron ejection cross sections. A comparison of the TOF results with previous measurements of Stolterfoht,[3] Crooks and Rudd,[8] and Toburen[9] is shown in Fig. 4 for 0.3 MeV proton ionization of nitrogen. The TOF spectra were normalized to the absolute cross sections at 50 eV where the agreement among previous measurements is excellent. The TOF spectra are in excellent agreement down to 2 eV with the results of Crooks and Rudd. Furthermore, if an integration over ejected electron energy and emission angle is performed to obtain the total ionization cross section, excellent agreement is obtained with the direct measurements of this quantity by Hooper *et al.*[10] The total ionization cross section obtained from the data of Toburen,[9] updated to conform to the spectral shape of TOF for electron energies less than 30 eV, is 3.1×10^{-16} cm^2 compared to 3.25×10^{-16} cm^2 obtained by Hooper *et al.*[10] Since the major portion of the total ionization cross section is contributed by low-energy electrons, this is excellent confirmation of our TOF spectral shape at low energies and lends confidence to the absolute values of the cross sections obtained with the electrostatic analysis at higher electron energies as well.

*This paper is based on work performed under United States Atomic Energy Commission Contract AT (45-1)-1830.

[1]M. Inokuti, Rev. Mod. Phys. 43, 297 (1971).
[2]M. E. Rudd and J. H. Macek, Case Stud. Atom. Phys. 3, 47 (1972).
[3]N. Stolterfoht, Z. Phys. 248, 92 (1971).
[4]N. Stolterfoht (private communication).
[5]Collimated holes structures are available through Technical Products Division, Brunswick Corp., 69 Washington St., Chicago, IL 60602.
[6]F. J. Comes, H. G. Sälzer, and G. Schumpe, Z. Naturforsch. 23, 137 (1968).
[7]K. Siegbahn, C. Nordling, G. Johansson, J. Hedman, P. F. Hedén, K. Hamrin, U. Gelius, T. Bergmark, L. O. Werme, R. Manne, and Y. Baer, *ESCA Applied to Free Molecules* (North-Holland, Amsterdam, 1969).
[8]J. B. Crooks and M. E. Rudd, Phys. Rev. A 3, 1628 (1971).
[9]L. H. Toburen, Phys. Rev. A 3, 216 (1971).
[10]J. W. Hooper, D. S. Harmer, D. W. Martin, and E. W. McDaniel, Phys. Rev. 125, 2000 (1962).